

# Reid's Paradox Revisited: The Evolution of Dispersal Kernels during Range Expansion

Benjamin L. Phillips,<sup>1,\*</sup> Gregory P. Brown,<sup>1</sup> Justin M. J. Travis,<sup>2</sup> and Richard Shine<sup>1</sup>

1. School of Biological Sciences, University of Sydney, Sydney, New South Wales 2006, Australia;

2. School of Biological Sciences, University of Aberdeen, Zoology Building, Tillydrone Avenue, Aberdeen AB24 2TZ, United Kingdom

---

**ABSTRACT:** Current approaches to modeling range advance assume that the distribution describing dispersal distances in the population (the “dispersal kernel”) is a static entity. We argue here that dispersal kernels are in fact highly dynamic during periods of range advance because density effects and spatial assortment by dispersal ability (“spatial selection”) drive the evolution of increased dispersal on the expanding front. Using a spatially explicit individual-based model, we demonstrate this effect under a wide variety of population growth rates and dispersal costs. We then test the possibility of an evolved shift in dispersal kernels by measuring dispersal rates in individual cane toads (*Bufo marinus*) from invasive populations in Australia (historically, toads advanced their range at 10 km/year, but now they achieve >55 km/year in the northern part of their range). Under a common-garden design, we found a steady increase in dispersal tendency with distance from the invasion origin. Dispersal kernels on the invading front were less kurtotic and less skewed than those from origin populations. Thus, toads have increased their rate of range expansion partly through increased dispersal on the expanding front. For accurate long-range forecasts of range advance, we need to take into account the potential for dispersal kernels to be evolutionarily dynamic.

**Keywords:** climate change, *Rhinella*, exotic species, introduced species, lag phase, nonequilibrium.

---

Understanding the process of range shift is of clear importance for estimating the impact of climate change (Thomas et al. 2004; Kokko and Lopez-Sepulcre 2006), delineating range edges (Bridle and Vines 2007), and managing invasive species (Mack et al. 2000). Basic theory indicates that species advance their ranges at a rate dependent on the distribution of dispersal distances in the

population, coupled with the population's rate of increase (Fisher 1937; Skellam 1951). More recently, however, it has been shown that the rate of advance of a population through space can be either constant or dynamic through time and depends on the interaction between population growth dynamics and the distribution of generational dispersal distances within a population (the dispersal kernel; Kot et al. 1996). These theoretical advances demonstrate that the rate of range advance can increase or decrease over time and that the most important factor determining the dynamics of range advance is the shape of the dispersal kernel (as opposed to the population's growth dynamics; Clark 1998). The dispersal kernel is ascendant because the shape of the dispersal kernel determines the per-generation spatial dynamics, and this, in turn, has important implications for the effect of population growth on the rate of range advance (Hastings 1996; Shigesada and Kawasaki 1997; but see Clark et al. 2001; Hastings et al. 2005). A general result of this body of theory is that highly kurtotic dispersal kernels (i.e., those with a “fat tail”) tend to generate range advances that are nonlinear, either accelerating or decelerating through time.

This body of theory, which we will refer to here as “static-kernel theory” has been successful at explaining observed patterns of range advance in both contemporary species invasions and range shifts observed in the fossil record, although usually the rate of advance has been underestimated (Hastings et al. 2005). In fact, static-kernel theory potentially explains Reid's paradox, the observation that the current dispersal ability of trees in the Northern Hemisphere seems too limited to explain the rate at which these trees recolonized areas of Europe and North America after the last ice age (Skellam 1951; Clark 1998; Clark et al. 1998). In 1998, Clark suggested that if an appropriate shape for the dispersal kernel is chosen (i.e., a fat-tailed distribution, where long-distance dispersal events are more common), the rate of advance of these tree species could indeed be explained by their current dispersal ability (albeit with some uncertainty associated with fitting the tail). Indeed, many kinds of invasion dynamics can be re-

\* Corresponding author; e-mail: bphi4487@mail.usyd.edu.au.

created, including constant and accelerating spread rates if the shape of the dispersal kernel is carefully chosen.

Despite its success, static-kernel theory has both theoretical and practical drawbacks. First, the theory predicts that with sufficiently fat-tailed kernels, the rate of range advance can accelerate infinitely, which is clearly not possible in the real world (Kot et al. 1996). Second, because the rate of advance is very sensitive to the shape of the tail of the distribution, it is critical to accurately fit this tail to observed data (Kot et al. 1996; Neubert and Caswell 2000). Unfortunately, fat-tailed dispersal kernels, by definition, are fat tailed because of rare long-distance dispersal events. The rarity of these events inevitably introduces a large error in estimating tail shape (Hastings et al. 2005). Thus, workers often are faced with a large possible range of tail shapes and thus a large range of possible range expansion dynamics.

These difficulties are not fatal to static-kernel theory; larger data sets and/or sensible bounds on tail shape can overcome them (see, e.g., Clark et al. 2001, 2003). In this article, however, we explore an overlooked extension to range expansion theory. We argue that dispersal kernels are unlikely to remain static during range expansion and that the process of range expansion itself drives rapid evolution of dispersal kernels. Thus, we suggest that static-kernel theory is likely to be accurate for only very short periods of range advance and that we need to incorporate the possibility of rapid evolution of dispersal kernels in order to advance our understanding of the way in which species shift their ranges.

Why do we expect dispersal kernels to shift during range advance? The shift is a natural consequence of range expansion and occurs because of a process that we refer to here as “spatial selection” (fig. 1). If we imagine a population where all the individuals disperse, then reproduce, and then die and that this population is placed into a large area of suitable vacant habitat, the population will advance its range as individuals disperse. Importantly, the process of dispersal effectively sorts individuals through space by dispersal ability (e.g., Hanski et al. 2002, 2004; Phillips et al. 2006). That is, individuals on the edge of the expanding population front are at that edge simply because they dispersed farther than other individuals in the population: the process of dispersal has spatially assorted the best dispersers in the population and placed them on the expanding front. Now, because all the best dispersers are in the same place at the same time, they will tend to breed with each other (the Olympic Village effect). Thus, if any component of dispersal ability is heritable in this hypothetical species, the offspring of the individuals on the front will tend to have higher dispersal ability than the offspring of individuals from the core of the population. If we imagine this process occurring every generation as

the population expands, the process of spatial assortment for dispersal ability behaves like a runaway evolutionary process, continually selecting for increased dispersal on the advancing front. Interacting with this process of spatial assortment are density effects. That is, individuals near the advancing front may benefit from a low-density environment (i.e., fewer conspecifics in their vicinity) and, as a consequence, leave more offspring. Thus, both density effects and spatial assortment on dispersal ability will interact to drive spatial selection and the evolution of increased dispersal ability on the expanding edge of range-shifting populations.

This process of spatial selection during range expansion was first described by Travis and Dytham (2002), who modeled a population expanding in discrete space. Here, we extend their model into continuous space and explore the shift in mean dispersal distance occurring as a consequence of range shift under a variety of conditions. We then go on to test the possibility of an evolved change in dispersal ability in a range-shifting species (the cane toad *Bufo marinus*) by measuring dispersal in individuals sampled from origin and frontal populations and tested in a common-garden field situation.

Cane toads were introduced into Australia in 1935 and have since colonized more than 1.2 million square kilometers of the continent (Urban et al. 2007). The rate at which they have colonized new areas has varied in time and space. Importantly, in the northern part of their range, like many invasive species (see Hengeveld 1989; Shigesada and Kawasaki 1997), cane toads have shown accelerating range advance: whereas they initially expanded their range at around 10 km/year, they now advance at more than 55 km/year (Phillips et al. 2006, 2007; Urban et al. 2008). Has this increase in the rate of range expansion occurred as a consequence of spatial selection?

## Methods

### *The Model: Population Description*

To examine the effect of spatial selection on the evolution of dispersal, we constructed a spatially explicit individual-based model in continuous space. To simplify the modeling process, reproduction was asexual and generations were discrete. The choice to model reproduction as asexual amplifies the spatial assortative mating effect (because assortative mating is absolute in space). In addition, our choice to model asexual reproduction will result in a slower rate of evolution than expected for sexuals with the same mutation rate, because different mutations in different individuals cannot be brought together in the same individual. The absence of recombination means that the asexual model may also require higher rates of mutation to pro-

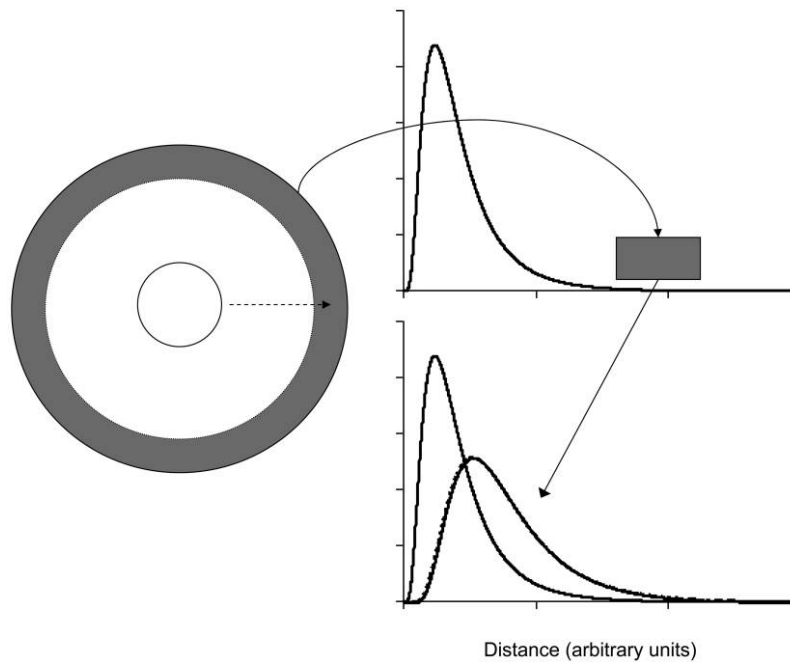


**Figure 1:** Spatial selection on dispersal distance during range expansion. A population's initial extent is represented by the inner circle, and its extent after a single generation of dispersal is shown by the outer circle. The graph on the top right represents the population's dispersal kernel (the distribution of per-generation dispersal distances in the population). After a single generation of dispersal, only the best dispersers will be on the population front (*shaded areas*). Given that these individuals are all in the same place at the same time, they will tend to breed with each other (assortative mating by dispersal ability). So if there is anything heritable about dispersal distance, the offspring of the individuals on the expanding front will have a dispersal kernel shifted to higher mean dispersal distances (*graph on bottom right*).

duce a given shift in dispersal ability. The model is thus minimally complex but should still capture the evolutionary dynamics of range expansion. Reproduction was modeled using logistic density dependence, with an expected number of offspring for each individual being dependent on the density of individuals in the surrounding area. Because individuals were distributed continuously, we calculated density by overlaying a grid on the population space, calculating the density of individuals in each grid cell, and assigning that density value to each individual in the cell (e.g., Dytham and Travis 2006). In an idealistic continuous-space model, the local density experienced by each individual is determined by calculating the number of individuals located within a zone of influence (Travis 2003 and references therein). However, the method we adopted represents a pragmatic compromise between the increased realism gained from the continuous-space approach and the computational efficiency of a grid-based description.

Following the calculation of population density, for each individual we calculated the expected number of offspring based on the formula  $E = \exp[r(1 - n/K)]$ , where  $E$  is the expected number of offspring for the individual,  $r$  is the

intrinsic growth rate of the population,  $n$  is the number of parents in the grid cell, and  $K$  is the per-cell carrying capacity. To introduce stochasticity into the reproductive process, the actual number of offspring per individual was achieved by drawing from a Poisson distribution with mean =  $E$ .

After reproduction, all offspring were given the opportunity to disperse, and all parents died. Individuals dispersed in random directions, with displacement calculated according to a correlated walk determined by three traits inherited from their parents: average distance moved per day (*distday*, excluding days where the animal does not move at all), probability of moving (*pmove*, the proportion of days in which an animal will move if given the opportunity), and diffusion (*diffn*, the circular diffusion of the animal's path). Our animals' path is a correlated walk (because each step depends on the value of the last via the diffusion parameter), but it is nonrandom in that we can calculate the exact displacement, given the individual's dispersal traits. The *diffn* parameter represents the length of the final displacement vector divided by the number of moves, where all moves are considered equal and one unit in length (Batschelet 1981), and is described as

$$\text{diffn} = \frac{\sqrt{(\sum_{i=1}^{i=N} \cos \theta_i)^2 + (\sum_{i=1}^{i=N} \sin \theta_i)^2}}{N},$$

where  $N$  is the number of moves and  $\theta$  represents the Cartesian angle of each move. The value of  $\text{diffn}$  varies between 0 and 1 and is effectively the proportion of the maximum displacement that an individual could achieve over a given number of equal steps. The value of  $\text{distday}$  was allowed to vary between 0 and  $\text{maxdist}/\text{numdays}$ , where  $\text{maxdist}$  is the maximum distance an organism can move in its lifetime and  $\text{numdays}$  is the number of days in which an animal has an opportunity to move. Inheritance was subject to mutation at a particular rate ( $\text{mutn}$ ) per trait, and to avoid complex assumptions regarding mutation, mutant traits were simply redrawn from a uniform distribution spanning the maximum and minimum trait values. Each individual had the opportunity to move for 100 days, and both the displacement and the total distance moved by the individual over these 100 possible steps were determined by reference to the individual's dispersal traits. In making these calculations, we assumed that individuals did not bias their walk in any particular direction; the predicted displacement over 100 days is thus  $100 \times \text{distday} \times \text{pmove} \times \text{diffn}$  (as for the telemetry data, see "The Data"). To calculate an individual's location at the end of 100 days of dispersal, we simply calculated the endpoint of the vector describing the displacement distance and a randomly chosen bearing.

We modeled perfectly reflecting boundaries at all edges of our simulated landscape. The total distance moved during dispersal ( $\text{TotDist}$ ) was calculated as  $\text{displacement}/\text{diffn}$ , and the probability of the individual surviving the dispersal episode was calculated relative to its  $\text{TotDist}$  via the "cost-of-dispersal" function  $f(\text{TotDist})$ . After successful dispersal, individuals were allowed to reproduce (relative to their new density), and the cycle of dispersal and reproduction began again.

The population was begun by an initial seed of 50% of the maximum number of individuals, each with a random value for each dispersal trait (selected from a uniform distribution). Thus, our initial distribution of displacement values in the population (being a multiple of these dispersal traits) was left skewed and approximately exponential (with an upper bound). The population was allowed to reach equilibrium through 100 generations in a finite population space ( $200 \times 200$ ; units arbitrary) before one edge of population space was opened and the population was allowed to disperse into this new homogeneous space ( $200 \times \infty$ ) for an additional 50 generations.

We ran this simulation model under several scenarios, modifying  $r$  (between 1.05 and 4.00),  $\text{mutn}$  (between 0 and  $10^{-2}$ ), and the dispersal cost function  $f(\text{TotDist})$ . We

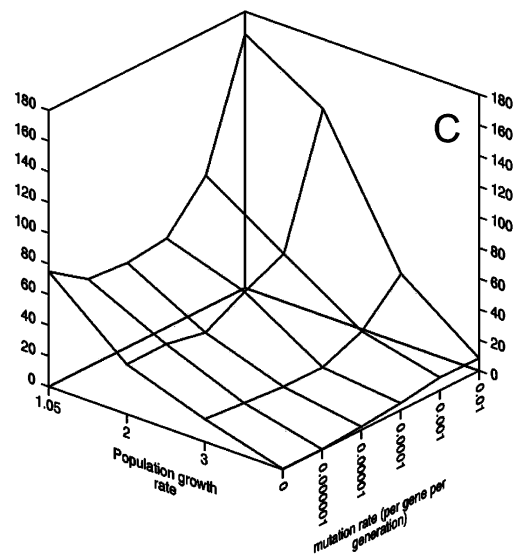
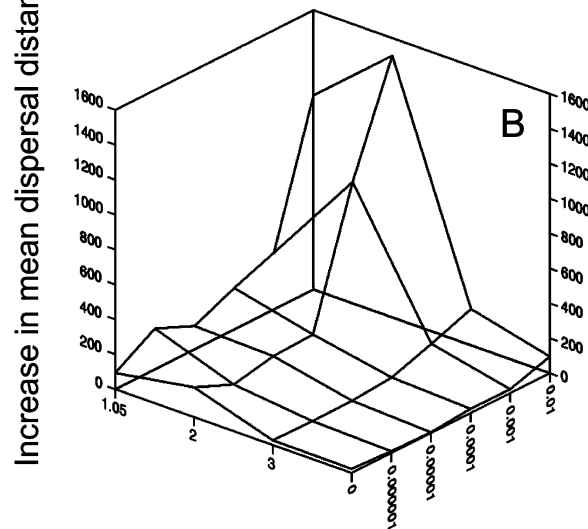
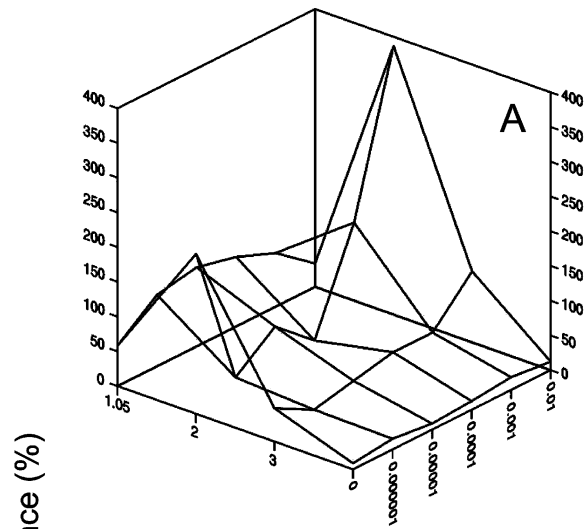
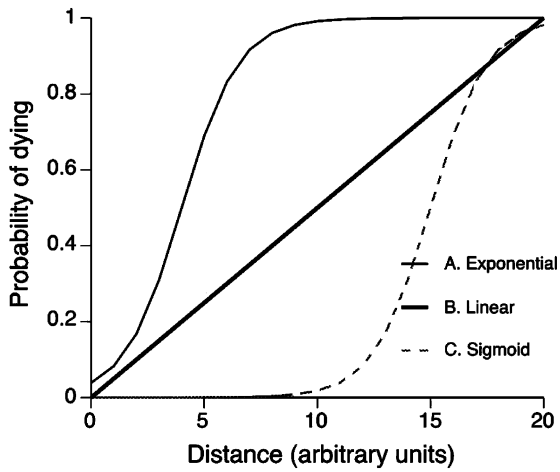
explored three potential shapes for the cost-of-dispersal function, using the flexible function described by Kun and Scheuring (2006). These functions were exponential, linear, and sigmoid (see fig. 2). For computational tractability, we kept our carrying capacity low and constant (20 individuals per grid cell, grid cell size  $10 \times 10$ ).

### The Data

After this general modeling exercise, we attempted to parameterize our model as closely as possible on the cane toad (*Bufo marinus*). In the northern part of their range, toads expanded their range naturally but were also artificially introduced ahead of the expanding population front between 1964 and 1968. These introductions were made to two towns on the Gulf of Carpentaria: Normanton and 160 km farther west at Burketown (fig. 3; Covacevich and Archer 1975; Floyd et al. 1981; Estoup et al. 2004; Urban et al. 2008). There is also evidence that an additional introduction was made about 50 km ahead of the advancing front near Burketown in 1979 (Freeland and Martin 1985).

An animal's rate of dispersal will depend not only on its intrinsic tendency to disperse but also on the environment in which it finds itself (Bowler and Benton 2005). Thus, to examine changes in intrinsic dispersal tendency through the invasion front, we sampled adult cane toads from four populations spanning the invasion history and measured their movement parameters in a common environment. Adult toads were collected from four sites spanning the invasion history: Cairns ( $16^{\circ}55'S$ ,  $145^{\circ}46'E$ , colonized 1936), Normanton, ( $17^{\circ}40'S$ ,  $141^{\circ}04'E$ , colonized 1966), Borroloola ( $16^{\circ}04'S$ ,  $136^{\circ}18'E$  colonized 1988), and Timber Creek ( $15^{\circ}38'S$ ,  $130^{\circ}28'E$ , colonized 2006; fig. 3). Sampled animals were each given a unique toe clip and brought to a common housing facility, where they were housed together for 2 months before the beginning of radiotelemetry.

Between January 7 and April 29, 2007 (the "wet season"), we released either four or eight animals per week at our study site on the Adelaide River floodplain at Middle Point, near Darwin ( $12^{\circ}38'S$ ,  $131^{\circ}19'E$ ; fig. 3). We generally released two individuals (one male and one female) from each population each week. Thus, each release event was balanced for population (except the last, where we had an uneven number remaining from each population) and for sex. Occasionally (at the beginning of the study), we released only four individuals, in which case these four represented one from each population and a single sex. At the end of the study, our total sample size was 89 individuals, all of which had been released at the same point. We attached radio transmitters to each animal via a belt (made of fine ball chain) around each animal's waist



(Brown et al. 2006; Phillips et al. 2007). The combined weight of transmitter and belt ranged between 3% and 12% of the animal's weight (mean = 6%). On the day after the animal's release, we began tracking and located each animal each day for the five days following release. Upon locating an animal, we recorded whether it was alive or dead and measured its locality to the nearest 10 m with a handheld GPS receiver. On the fifth day after release, each animal was captured and placed back into the common housing facility. Previous radio-tracking work on toads suggests that they do not behave any differently in the first days of tracking than in subsequent days (G. P. Brown, unpublished manuscript).

At the completion of radio tracking, we derived three movement parameters for each individual that were exactly homologous to the dispersal traits used in our model: mean daily distance moved (distday, the sum of all daily movement distances divided by the number of days where the daily movement distance was greater than 0), probability of moving (pmove, the number of days where daily movement distance was greater than 0 divided by the total number of tracking days), and diffusion (diffn, the circular diffusion of the animal's path, calculated as in "The Model: Population Description"). Using these parameters, we can construct a predicted displacement ( $\text{disp}_n$ ) for each individual over any number of days, calculated simply as  $\text{disp}_n = \text{numdays} \times \text{distday} \times \text{pmove} \times \text{diffn}$ , where numdays is the number of days of potential movement.

#### The Parameterized Model

In the case of cane toads, we ran the model over 72 generations of expansion (one generation = 1 year), with a slightly increased carrying capacity of 30 per grid cell. We set the spatial units in the model to kilometers, so the equilibrium population evolved for 100 generations in a  $200 \times 200$ -km area before being allowed to expand into a  $200 \times \infty$  area. The cost of dispersal,  $f(\text{TotDist})$ , was calculated as the sum of two curves. The first curve was a simple linear relationship between TotDist and the probability of dying ( $P(\text{die})$ ), which reached a value of 1 at an empirically determined maximum dispersal distance of 113 km/year (being the maximum distday value we observed across all our study animals, multiplied by 180, the length of the wet season and thus the approximate number of days per year available to toads to disperse; Phillips et al. 2007). This linear relationship reflects unspecified costs

of movement (e.g., from predation other than birds, energetic costs, reproductive costs) and assumes simply that an individual increases its chance of dying (or decreases its chance of reproducing) in proportion to the distance it moves. The second curve reflected an empirically determined relationship between predation rate and distance moved (see "Results"). The probability of mortality during dispersal was set as the sum of these two curves (and any probability greater than 1 was reduced to a probability of 1); thus,  $f(\text{TotDist})$  describes the risk of predation coupled with the energetic cost associated with dispersal: individuals that disperse to the maximum degree possible leave no offspring, either because they have died or because they have no remaining energy for reproduction (and given the discrete generations in the model are thus effectively dead).

## Results

### The General Model

*The General Model at Equilibrium.* All runs were conducted under the same value of  $K$  (per-cell carrying capacity) because preliminary analysis showed that variation in  $K$  had no major effect on the rate of population spread in our model (fig. 4). Normally,  $K$  may influence the rate of advance simply because a greater number of individuals implies a greater chance of a long-distance dispersal event. However, because individuals in our model had fixed values for dispersal traits (and we did not draw dispersal distance randomly from an individual-level distribution), this effect of  $K$  is minimized.

All runs rapidly (usually within five generations) reached equilibrium levels of lifetime dispersal distance during the 100 generations of evolution in the finite habitat space. The rapid equilibration was due to the large standing variation on which selection could act because the space was initially seeded with random uniform distributions of dispersal traits. Equilibrium levels of dispersal were related strongly to the population growth rate ( $r$ ), with higher values of  $r$  leading to the evolution of greater equilibrium dispersal distances. The mutation rate had no effect on equilibrium values of dispersal.

To illustrate the general results obtained in the model, we show and discuss a model parameterized with real distances and the toad cost-of-dispersal function (see "The Predation Cost of Dispersal"), but results using other dispersal-cost functions were qualitatively similar (see fig. 2).

---

**Figure 2:** General model results: percentage increase in mean dispersal distance between frontal and origin populations after 50 generations of range expansion. Three dispersal costs were modeled across a range of values for population growth ( $r$ ) and per-generation mutation rate (mutn). The left-hand panel shows the three functions describing dispersal cost, and A, B, and C show the percentage increases in mean dispersal ability and the way this varies with both  $r$  and mutn. Note that the percentage increase in mean dispersal distance is always positive.

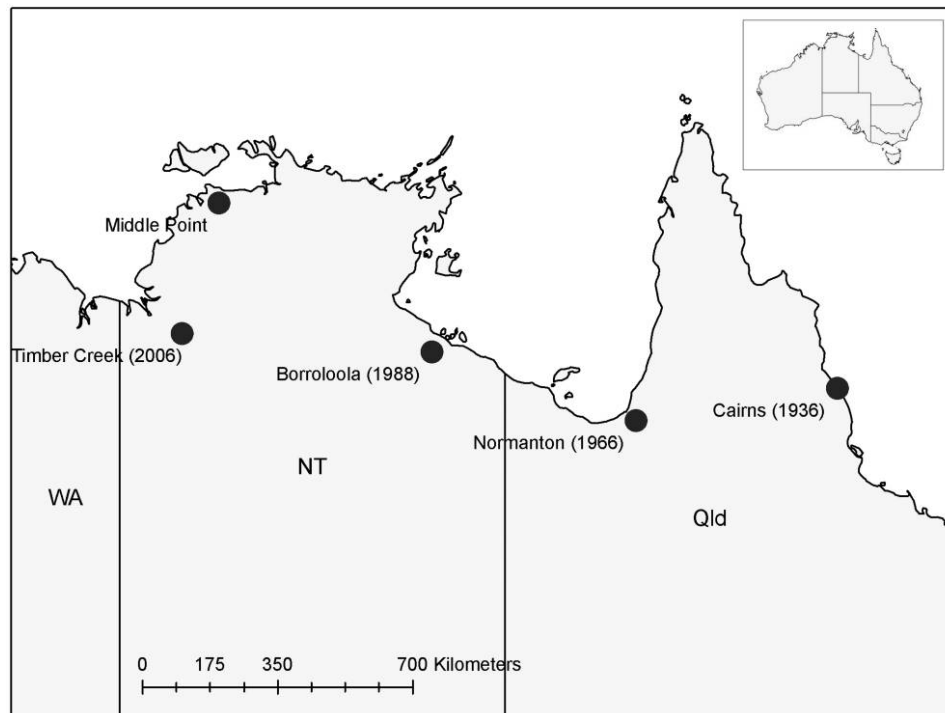
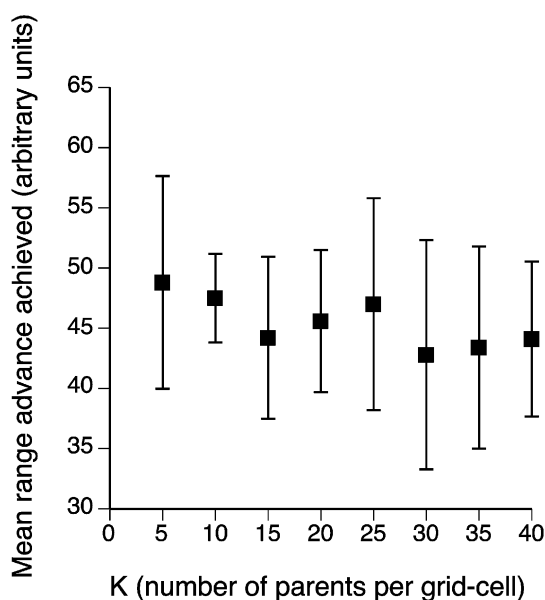


Figure 3: Populations from which toads were sampled. Toads were introduced near Cairns and have spread westward to Timber Creek. The year of toad colonization is given in parentheses.

First, equilibrium values for dispersal were not qualitatively different from values obtained at the population origin after 50 generations of range expansion. Thus, origin populations do not appear to be greatly affected by spatial selection occurring on the moving invasion front. The lower gray surface in figure 5 thus illustrates the effects of intrinsic population growth rate ( $r$ ) and mutation rate (mutn) on the equilibrium level of individual displacement for a model parameterized with real distances and the toad-specific cost-of-dispersal function. Each point on the surface reflects the average displacement across a sample of individuals in the original space, averaged across five model runs. Clearly,  $r$  has a major influence on equilibrium dispersal distances, whereas the mutation rate has almost no influence (as stated above). The effect of  $r$  on equilibrium dispersal reflects the influence of density dependence in this system. When  $r$  is high, there is a large reproductive advantage to be gained by individuals dispersing into “vacant” habitat, whereas when  $r$  is low, the advantage of dispersing is relatively small. At  $r = 1.05$ , for example, an individual gains only a 5% increase in reproductive output if it successfully disperses to vacant habitat—an advantage too small to compensate for the high costs associated with dispersal.

*The General Model during Range Expansion.* During range expansion, all models showed an increase in mean dispersal distance on the front compared with that for the origin population (figs. 2, 5, 6). This increase could result from numerous strategies, and the exact strategy that evolved often depended on where mutations occurred (e.g., fig. 6). This increased level of dispersal was true for all dispersal-cost functions tested and across all levels of  $r$  and mutn tested, but the percentage increase in mean dispersal ability tended to be greatest at low to intermediate levels of  $r$  (between 1.05 and 2.5; fig. 2). This result probably reflects the fact that high  $r$  generates high dispersal at equilibrium and thus limits the potential for increased dispersal to evolve. Interestingly, dispersal was driven upward so forcefully that there was rarely any variation in dispersal distance remaining on the advancing front (fig. 6). The zero remaining variance in dispersal is a pathology of the model and is unlikely to be realized in nature but nonetheless does indicate that dispersal has been strongly selected.

Figure 5 shows the effect of range expansion on the evolution of dispersal in the semiparameterized model. In this figure, the lower surface represents displacement values averaged across all individuals within 50 km of the



**Figure 4:** Effect of  $K$  on the rate of population advance. These data come from replicated simulations where  $r = 3$ ,  $\text{mutn} = 10^{-5}$ , dispersal costs are linear, and there are 50 generations of range expansion.  $K$  was allowed to vary between 5 and 40, with 10 replicate simulations at each value of  $K$ . Error bars represent 2 SD.

origin, whereas the upper surface represents displacement values averaged across all individuals within 50 km of the expanding population front. At all values of  $r$  and  $\text{mutn}$ , displacement is higher on the front than in the origin population. In addition, frontal displacement values are clearly influenced by both  $r$  and  $\text{mutn}$ . This result reflects the two processes contributing to spatial selection: spatial assortment by dispersal ability and density-dependent fecundity. Density-dependent fecundity (or survivorship) influences maximal dispersal values because it sets the level of benefit derived by individuals that achieve the vacant frontal habitat; individuals dispersing ahead of the front receive a reproductive benefit directly proportional to  $r$ . When  $r = 4$ , for example, there is a fourfold reproductive advantage to occupying vacant habitat, and this massive advantage pushes frontal dispersal levels up to where the probability of surviving dispersal is less than 40%. We also note that even when the mutation rate is 0 and  $r$  is very low (1.05), there is a difference in dispersal ability between the front and origin populations. Because the mutation rate is 0, this difference in dispersal ability is primarily a consequence of spatial assortment (with very weak density effects) acting only on standing variation, and it is as close as we can come to removing the advantageous effect of low density from our model. If, in figure 5, we view the force of spatial assortment as constant in all range expan-

sion models (and the lower gray surface as the result with no spatial assortment), then we can see that spatial assortment interacts with both density effects (because high  $r$  levels depart more rapidly from the null surface) and mutation rate (because high mutation departs more rapidly from the null surface). Furthermore, the skewed nature of the upper surface describing the effect of  $r$  and  $\text{mutn}$  on frontal dispersal clearly indicates an interaction between these two factors in their effect on spatial selection.

### Toad Movement Results

*Population Comparisons.* There was no significant difference across populations in the mean body size (snout-urostyle length) of the toads tracked ( $F = 1.03$ ,  $\text{df} = 1, 88$ ,  $P = .38$ ). Nonetheless, comparison of movement parameters from toads spanning the invasion history (from long-established populations to still-expanding populations) reveals clear trends in all movement-related parameters. Across all measures of individual movement, frontal animals tended to disperse the farthest, with decreasing dispersal ability related to distance from the front (see fig. 7). After normalizing transformations, these linear regressions were significant or near significant for the

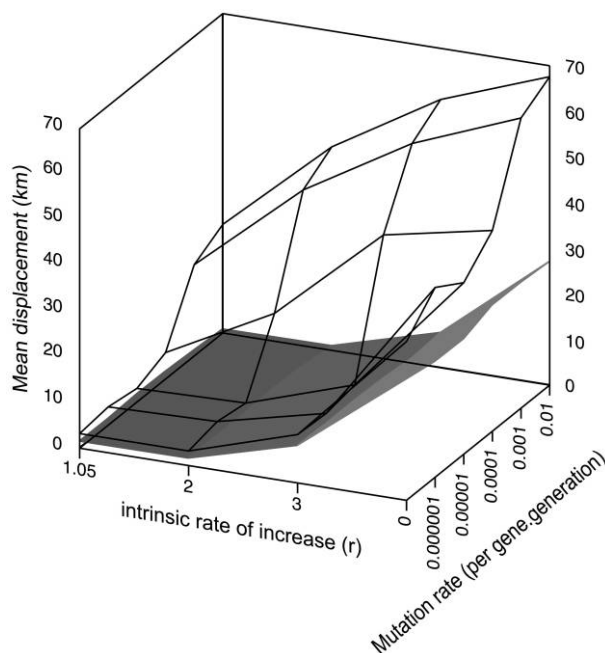
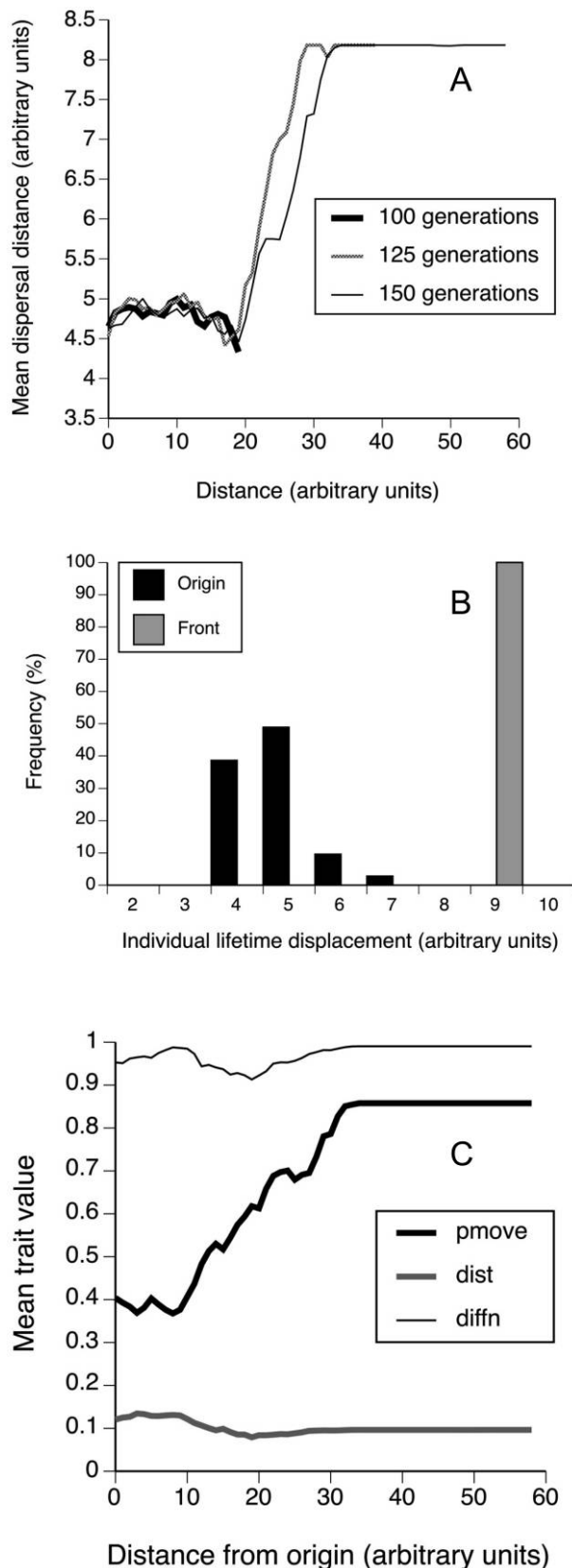


**Figure 5:** Semiparameterized model. Effect of  $r$  and mutation rate ( $\text{mutn}$ ) on displacement (km/year) at the origin and at the front. Frontal values are shown by the lattice, whereas origin values are illustrated with the gray surface.





probability of moving ( $F = 8.25$ ,  $df = 1, 87$ ,  $P = .005$ ), the mean distance moved per night ( $F = 8.98$ ,  $df = 1, 87$ ,  $P = .004$ ), the circular diffusion ( $F = 3.80$ ,  $df = 1, 70$ ,  $P = .055$ ), and finally, the mean displacement per night ( $F = 10.39$ ,  $df = 1, 87$ ,  $P = .002$ ). Frontal toads tend to move more often, move farther when they do move, and follow straighter paths than toads from old populations.

To examine the effectiveness of the combined movement parameters ( $pmove$ ,  $distday$ , and  $diffn$ ) in predicting actual displacement, we plotted  $\ln$ -transformed actual displacement values against those predicted by the simple multiplication of all movement parameters with the number of nights of observation (also  $\ln$  transformed). The resulting regression was reasonably tight ( $R^2 = 0.64$ ), the intercept was not significantly different from 0 (one-tailed randomization test:  $P = .31$ , indicating a slope not different from 1 in the untransformed data), and the observed slope ( $b = 0.87$ ) was not significantly less than 1 (one-tailed randomization test:  $P = .362$ , indicating an exponent not different from 1 in the untransformed data). Deviations from a perfect fit are probably caused by slight turn biases in real toads; nonetheless, our basic movement parameters predicted toad displacement with reasonable accuracy.

Using these results, we were able to predict the displacement per toad over 180 days of dispersal (which is the approximate number of days per year when wet climatic conditions enable toad dispersal in northern Australia). The resulting yearly dispersal kernels are shown in figure 8. Importantly, the kurtosis (or tail fatness) of these distributions increased with distance from the invasion front: toad populations on the front appear to have flatter, more symmetrical, and thinner-tailed dispersal kernels than toads from older populations (fig. 8). The relationships between skewness, kurtosis, and distance were nearly significant in both cases (skewness:  $F = 30.08$ ,  $df = 1, 2$ ,  $P = .032$ ; kurtosis:  $F = 15.10$ ,  $df = 1, 2$ ,  $P = .060$ ).

*The Predation Cost of Dispersal.* During the course of radio

**Figure 6:** A typical model run ( $r = 3$ ,  $mutn = 10^{-5}$ ,  $K = 20$ , linear dispersal cost,  $maxdist = 20$ ). **A** shows a snapshot of the entire population at three time periods: 100 generations (the equilibrium situation), 125 generations (25 generations of range expansion), and 150 generations (50 generations of range expansion). The Y-axis shows mean lifetime dispersal distances for individuals at that distance. **B** shows the dispersal kernel that evolves at the origin and advancing front after 50 generations of dispersal. There is no variance for dispersal distance on the expanding front. **C** shows the shift in trait values through space after 50 generations of range advance. In this case, a genotype conferring high diffusion ( $diffn$ ) and high probability of moving ( $pmove$ ) has developed on the front, but other strategies are possible.

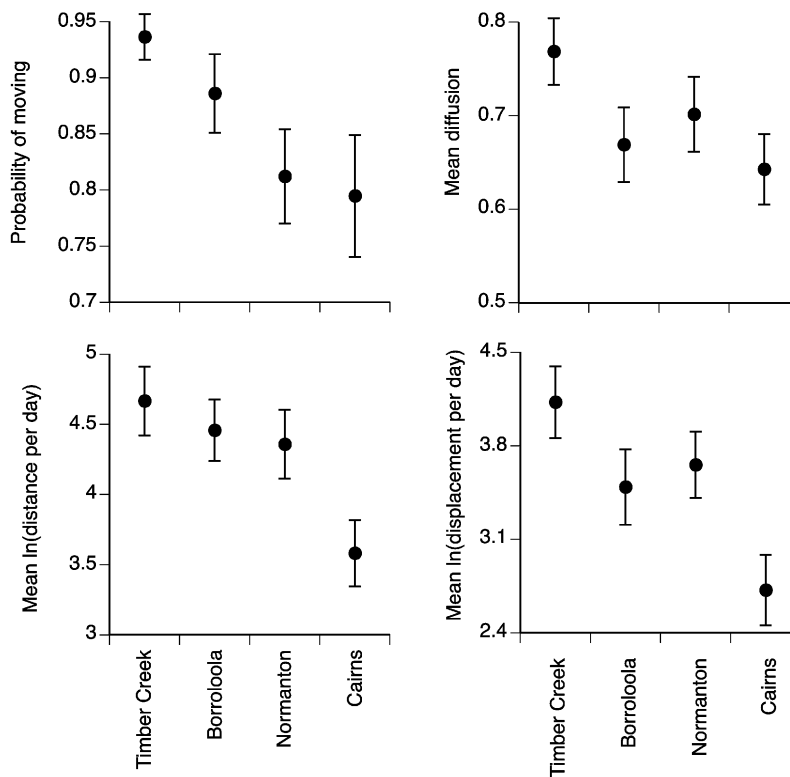


**Figure 7:** Sampling localities and the effect of invasion history on dispersal attributes of 89 cane toads. All dispersal parameters show increased values on the invasion front (Timber Creek), leading to a net decline in individual displacement with distance from the invasion front. All toads were radio tracked at Middle Point (see fig. 3).

tracking, five of our 89 animals were killed by predators (four by birds and one by rats). The probability of an individual being killed by a predator was positively associated with the predicted 5-day total distance moved by the toad (we used predicted 5-day distance because we rarely had 5 days of data on predator-killed animals: logistic regression  $\chi^2 = 5.32$ ,  $df = 1$ ,  $P = .02$ ). We thus used the logistic regression to predict the probability of an individual being killed by a predator as a function of distance. To scale this relationship up to 180 days of movement, we simply iterated/multiplied the logistic regression function by  $180/5 = 36$ . Thus, the predation cost of dispersal was approximated as

$$P(\text{die}) = \frac{36}{1 + \exp[-0.437 \ln(\text{TotDist}/36) + 6.735]}$$

When this function was added to the linear function describing a linear likelihood of surviving (for other reasons), the resulting curve was convex but approximately linear (fig. 9).

#### *The Toad-Parameterized Model*

Cane toads reach high densities in nature (more than 2,000/ha in some cases; Freeland 1986; Lampo and De Leo 1998; but given that these estimates come from breeding areas, toads probably exist at much lower average densities than this), while the density in our model is equivalent to 0.003 animals/ha. Unfortunately, setting realistic values for  $K$  would have required the simulation of billions of individuals at a time, which was computationally intractable. The low values of  $K$ , coupled with the fact that our model describes an asexual organism, mean that our toad-parameterized model is unlikely to accurately reflect real values for  $r$  or  $\text{mutn}$  in the toad population. Thus, we restrict ourselves here to demonstrating that the shift in mean rate of dispersal in toads can be easily explained by spatial selection and that this shift causes accelerating range advance.

*Estimating  $r$ ,  $\text{mutn}$ , and the rate of advance.* We determined values of  $r$  and  $\text{mutn}$  that best describe the toad system. To do this, we first estimated the mean for 180-day displacement of frontal (Timber Creek, 21.0 km/year) and origin (Cairns, 6.6 km/year) radio-tracked toads.

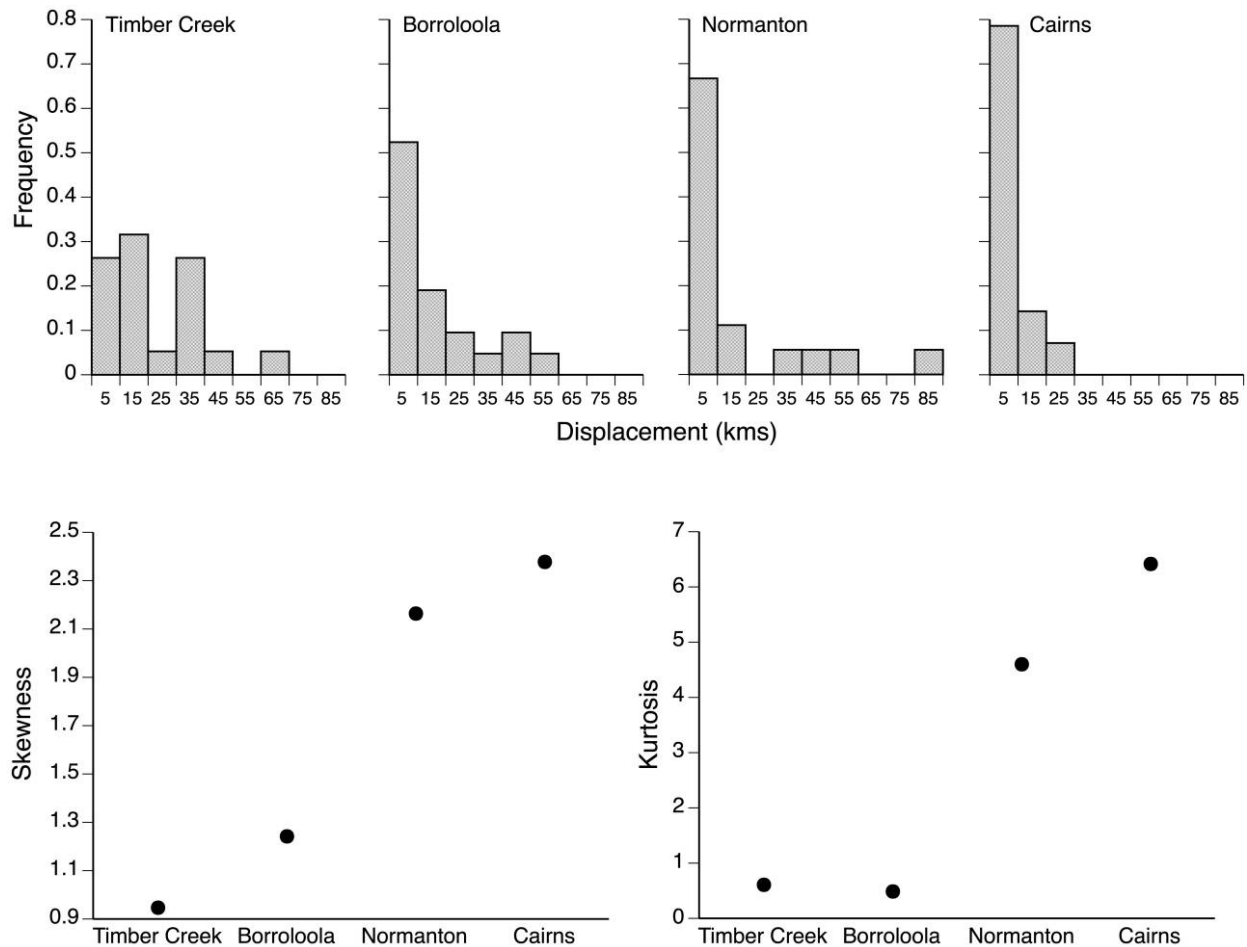


**Figure 8:** Change in the shape of the distribution of toad yearly dispersal distances. Histograms show four populations, from the invasion front (Timber Creek) to the origin (Cairns) populations. Lower panels show change in skewness and kurtosis as a function of distance from the front.

These means were then visualized as contours on the cubic-spline surfaces describing 180-day displacement of our “virtual toads” as a function of  $r$  and  $\text{mutn}$ . The intersection of these contour lines gave the values in parameter space that best describe the toad model (i.e., the combination of values that evolved both the equilibrium and frontal rates of dispersal:  $r \approx 2.8$ ,  $\text{mutn} \approx 3 \times 10^{-5}$ ). Thus, we chose values of  $r$  and  $\text{mutn}$  that, within the model, produced a shift in mean dispersal distance similar to that observed in our radio-tracking study. We used these values to examine changes in the rate of advance that could occur if spatial selection is occurring. Using these parameter values, we ran 100 simulations of the model to determine the average relationship between range extent and time. These simulations showed a clearly accelerating rate of range advance that, nonetheless, lagged behind the observed rate of spread (fig. 10). This lag occurred even if we explicitly modeled the artificial introduction of toads

ahead of the front (by introducing 20 individuals from the front to an appropriate place ahead of the front; fig. 10), as happened around Normanton and Burketown between 1964 and 1968 (Covacevich and Archer 1975; Sabath et al. 1981), with the model falling approximately 460 km short of the range extent achieved by real toads.

### Discussion

Our general model shows that range expansion causes “spatial selection,” which drives the evolution of increased dispersal on the expanding front. This result appears true over a wide range of dispersal costs, population growth rates, and mutation rates (figs. 2, 3). Thus, the null expectation is that species expanding their range will evolve increased dispersal ability on the expanding front. Certainly, when we tested this possibility in cane toads in Australia, we found a significant increase in toads’ dis-

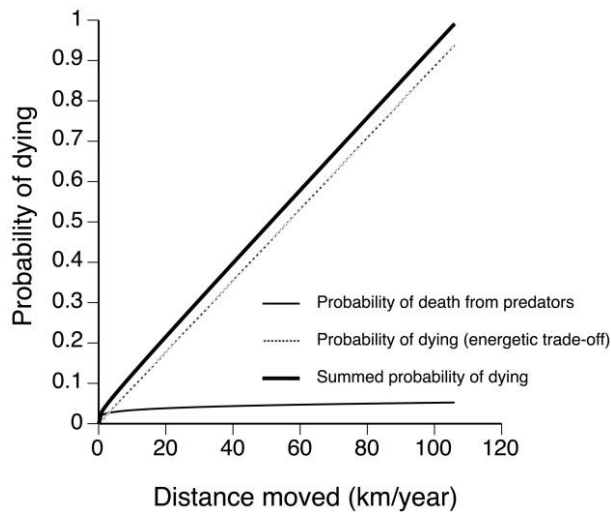


**Figure 9:** Cost-of-dispersal function for cane toads. This function is the sum of two curves, one describing the probability of predation with movement distance and the other being a simple linear relationship between distance moved and probability of dying.

persal rates with distance from the introduction point. Toads from frontal populations tended to move farther than those from long-established populations, with intermediate populations showing intermediate dispersal distances (fig. 7). While our design cannot prove that these changes are genetic, the fact that there was no significant difference in mean body size between populations and that all toads were housed in a common environment for 2 months (and then radio tracked contemporaneously in the same location) suggests that the differences may well have a genetic basis.

The effect of spatial selection on dispersal ability was so strong that, in the general model, there was greatly reduced variation in dispersal distance remaining after 50 generations of range expansion. Thus, spatial selection either selects the best dispersers in a population (standing variation only) or also captures highly dispersive mutants that arise near the expanding front. Our data on cane toads showed clear shifts in the dispersal kernel as a consequence of invasion history. Frontal toad populations not only had higher mean dispersal distances (as predicted by our general model) but also had less kurtotic and less skewed dispersal kernels (which our model was unable to simulate). The shift in shape of the toads' dispersal kernel appears consistent with strong directional selection on dispersal ability.

Static-kernel theory argues that accelerating range advance is best explained by fat-tailed, kurtotic dispersal kernels. We can, however, suggest a clear alternative: dispersal rate evolves upward on the expanding front. In toads, this

increase in dispersal is manifested in a shift in the shape of the dispersal kernel as well as in an increase in mean dispersal. Importantly, in toads the dispersal kernel becomes less kurtotic and less skewed. Given that toads now advance their range at more than five times their historical speed (Phillips et al. 2006; Urban et al. 2008) and appear to be doing so with thinner-tailed kernels, our results suggest that evolved shifts in dispersal distance on the expanding front may (in the long term) be a stronger driver of expansion dynamics than just the shape of the (initial) dispersal kernel. Our results, therefore, suggest that dispersal kernels are evolutionarily dynamic and respond rapidly and predictably to range advance.

Using evolutionarily dynamic kernels to model range advance would have several advantages. First, the evolutionary framework prevents infinitely increasing range advance, as can occur with sufficiently fat-tailed dispersal kernels under static-kernel theory (Kot et al. 1996). The reason for this is that, by explicitly incorporating trade-offs through the cost of dispersal function, the evolutionary model sets a natural upper limit to dispersal distance and thus the rate of range advance. Second (and more speculatively), the evolutionarily dynamic-kernel approach probably erodes the sensitive dependence of expansion dynamics on the shape of the tail of the dispersal kernel. The reason for this is that, in addition to being

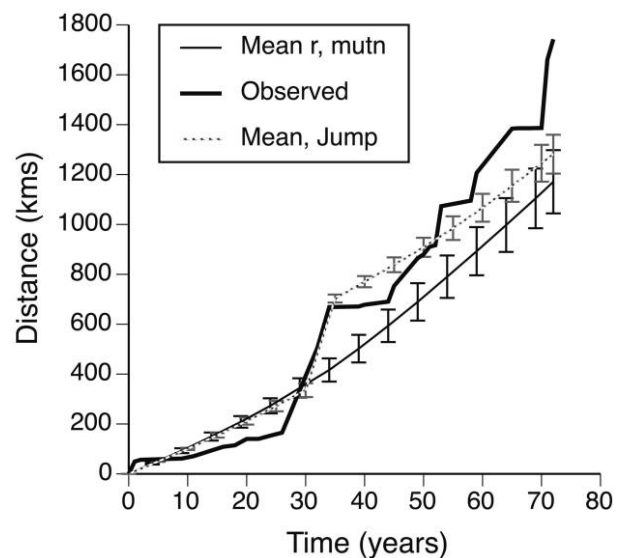


**Figure 10:** Predicted and observed rates of invasion of cane toads in northern Australia. Data for the predicted rate of spread come from 100 runs of the parameterized model under two scenarios. Scenario 1 is simple continuous range expansion. Scenario 2 incorporates known history, in that toads were introduced to Normanton and Burketown ahead of the invasion front in 1964–1968. Observed rates of spread come from Urban et al. (2008). Error bars represent 2 SD.

naturally constrained by trade-offs, the shape of the dispersal kernel on the advancing front shifts very rapidly; fat-tailed kernels will not remain fat tailed for long because the initially rare long-distance dispersers will rapidly become the dominant phenotype on the expanding front. Thus, rare long-distance dispersal remains important to measure, but it does so because it gives us an indication of the potential for the kernel to shift rather than because of its influence on the initial tail shape and short-term expansion dynamics.

When we parameterized our model for the toad system, our model predicted a clear acceleration in the rate of range advance (fig. 10). Nonetheless, the model's predicted rate of advance still fell short of the observed rate of advance. This is a common outcome of static-kernel models also, where insufficient sampling of rare long-distance dispersal is invoked as a likely explanation (Hastings et al. 2005). In our case, we doubt that insufficient sampling is the cause of our discrepancy. The reason for this is that we measured dispersal directly (using radiotelemetry) and were able to sample a population where dispersal appears to have been selected upward for approximately 70 generations. Thus, while we may have underestimated potential dispersal in toads, we doubt that we have underestimated it by much. Instead, we suggest that the discrepancy between our observed and predicted rates of range advance is a direct consequence of the simplicity of our model. First, the strength of spatial selection on dispersal ability in our model was so strong that our model eroded all variation in dispersal distance on the front. Thus, our mean dispersal distance on the front was also our maximum dispersal distance on the front. This problem could be corrected by increasing the complexity of the genes coding for dispersal or by introducing sexual reproduction. Alternatively, if every individual carried its own dispersal kernel (from which it randomly chooses a dispersal distance), we could ensure that a more realistic population dispersal kernel would exist on the expanding front. Future work will resolve this issue.

A second possible reason for the lower rate of range advance in the model may involve the shape of the density dependence function. Alternative density dependence functions are obviously possible (e.g., Allee effects or negative Allee effects), and such effects can modify not only the rate at which a population advances (Taylor and Hastings 2005; Johnson et al. 2006; Tobin et al. 2007) but also the rate at which a population shifts its dispersal traits in response to spatial selection (Travis and Dytham 2002).

A final potential reason for the discrepancy between modeled and observed range advance is that the model assumes a static value for traits other than dispersal, most notably the population growth rate ( $r$ ), carrying capacity ( $K$ ), and the number of days of dispersal (numdays). In

reality, all of these traits will vary through both space and time. Through space, attributes of the environment will have a clear effect on  $r$ ,  $K$ , and numdays such that populations living in a more suitable environment may have higher values for all of these parameters. One way to incorporate such spatial variation would be to use mechanistic predictions of habitat suitability, as generated by physiological models such as those of Kearney and Porter (2004), to index values of population growth and dispersal parameters. The rate of population increase,  $r$ , will also vary through time, potentially as a consequence of selective forces operating on the front in a way similar to those operating on dispersal. Certainly, the idea that invasive populations are " $r$  selected" is an old one (e.g., Lewontin 1965). If  $r$  is evolving upward at the same time as dispersal ability, then the rate of advance estimated by our current model will always be an underestimate (Holt et al. 2006). The fact that we observe only a threefold increase in mean dispersal distance (coupled with a decreased kurtosis in the kernel) but also a fivefold increase in the rate of range advance suggests that changes in dispersal ability alone will not be able to account for the rate of range advance that we currently observe in toads in northern Australia; it seems likely that  $r$  is shifting.

There is considerable scope for future work to assess how realistic patterns of movement behavior should evolve in relation to landscape structure and the nature of population dynamics (e.g., Hovestadt et al. 2001) as well as range expansion. In this work, a major challenge will lie in gaining robust empirical estimates for the cost of dispersal. The cost of dispersal obviously plays a pivotal role in constraining the evolution of dispersal, yet obtaining good information on direct and indirect costs of dispersal is not a trivial undertaking because dispersal costs potentially have many sources and may act at various life-history stages. In the present case, we have assumed that the cost of dispersal comes from two sources, one that we have measured (predation on adults) and one that we have been forced to assume (energetic and other costs). Although our assumption of a linear energetic cost of dispersal may or may not be an accurate representation, the real curve for toads is very likely to fall within the bounds we explored in the general model. Thus, we can be reasonably confident that toads have indeed experienced spatial selection on dispersal ability (because the general model always gave an increase in mean dispersal distance, irrespective of the cost function). However, the exact rate and magnitude of the ultimate shift in dispersal distance achieved by toads may vary, depending on how we represent the cost of dispersal.

In summary, we show that evolved shifts in dispersal kernels appear to be a natural consequence of the dynamics of range expansion. To make robust forecasts of range

advance in either invasive species or natives shifting their range in response to climate change, we need to take the evolutionarily dynamic nature of dispersal kernels into account. Doing so resolves potential problems with current range-advance theory, potentially explains the ubiquitous lag phase seen in the expansion rate of invasive species, and generates an alternative explanation for Reid's paradox. To explain Reid's paradox, we simply need to acknowledge that the historical spread rate of trees after the last ice age was a function of a dispersal kernel that was subject to spatial selection as the trees advanced. Trees on the expanding front probably evolved increased seed dispersal and thus drove the front forward at an increasing rate. The dispersal kernel we measure in trees today may simply be an indication of the kernel that evolves under range shift.

### Acknowledgments

We would like to thank M. Greenlees, J. Llewelyn, and J. Smith for assistance with the collection of toads, as well as E. Cox and J. Stevens for endless field support. We also thank S. Baird, A. Estoup, and M. Urban for entertaining and stimulating discussions. M. Urban provided the observed data on the rate of toad spread from an unpublished manuscript, and A. Estoup provided comments on an earlier draft. The modeling component would not have been possible without the assistance of an Environmental Futures Network grant to B.L.P. for travel to the United Kingdom. Additional funding was provided by Australian Research Council grants to B.L.P. and R.S.

### Literature Cited

- Batschelet, E. 1981. Circular statistics in biology. Academic Press, New York.
- Bowler, D. E., and T. G. Benton. 2005. Causes and consequences of animal dispersal strategies: relating individual behaviour to spatial dynamics. *Biological Reviews* 80:205–225.
- Bridle, J. R., and T. H. Vines. 2007. Limits to evolution at range margins: when and why does adaptation fail? *Trends in Ecology & Evolution* 22:140–147.
- Brown, G. P., B. L. Phillips, J. K. Webb, and R. Shine. 2006. Toad on the road: use of roads as dispersal corridors by cane toads (*Bufo marinus*) at an invasion front in tropical Australia. *Biological Conservation* 133:88–94.
- Clark, J. S. 1998. Why trees migrate so fast: confronting theory with dispersal biology and the paleorecord. *American Naturalist* 152:204–224.
- Clark, J. S., C. Fastie, G. Hurr, S. T. Jackson, C. Johnson, G. A. King, M. Lewis, et al. 1998. Reid's paradox of rapid plant migration. *BioScience* 48:13–24.
- Clark, J. S., M. Lewis, and L. Horvath. 2001. Invasion by extremes: population spread with variation in dispersal and reproduction. *American Naturalist* 157:537–554.
- Clark, J. S., M. Lewis, J. S. McLachlan, and J. HilleRisLambers. 2003. Estimating population spread: what can we forecast and how well? *Ecology* 84:1979–1988.
- Covacevich, J., and M. Archer. 1975. The distribution of the cane toad, *Bufo marinus*, in Australia and its effects on indigenous vertebrates. *Memoirs of the Queensland Museum* 17:305–310.
- Dytham, C., and J. M. J. Travis. 2006. Evolving dispersal and age at death. *Oikos* 113:530–538.
- Estoup, A., M. Beaumont, F. Sennedot, C. Moritz, and J.-M. Cornuet. 2004. Genetic analysis of complex demographic scenarios: spatially expanding populations of the cane toad, *Bufo marinus*. *Evolution* 58:2021–2036.
- Fisher, R. A. 1937. The wave advance of advantageous genes. *Annals of Eugenics* 7:355–369.
- Floyd, R. B., W. C. Boughton, S. Easteal, M. D. Sabath, and E. K. van Beurden. 1981. The distribution records of the marine toad (*Bufo marinus*). 1. Australia. Australian Environmental Studies Working Paper 3/81. Griffith University, Brisbane.
- Freeland, W. J. 1986. Populations of cane toad *Bufo marinus* in relation to time since colonization. *Australian Wildlife Research* 13:321–330.
- Freeland, W. J., and K. C. Martin. 1985. The rate of range expansion by *Bufo marinus* in northern Australia 1980–84. *Australian Wildlife Research* 12:555–560.
- Hanski, I., C. J. Breuker, K. Schöps, R. Setchfield, and M. Nieminen. 2002. Population history and life history influence the migration rate of female Glanville fritillary butterflies. *Oikos* 98:87–97.
- Hanski, I., C. Erälahti, M. Kankare, O. Ovaskainen, and H. Sirén. 2004. Variation in migration propensity among individuals maintained by landscape structure. *Ecology Letters* 7:958–966.
- Hastings, A. 1996. Models of spatial spread: a synthesis. *Biological Conservation* 78:143–148.
- Hastings, A., K. Cuddington, K. F. Davies, C. J. Dugaw, S. Elmendorf, A. Freestone, S. Harrison, et al. 2005. The spatial spread of invasions: new developments in theory and evidence. *Ecology Letters* 8:91–101.
- Hengeveld, R. 1989. Dynamics of biological invasions. Chapman & Hall, New York.
- Holt, R. D., M. Barfield, and R. Gomulkiewicz. 2006. Theories of niche conservatism and evolution: could exotic species be potential tests? Pages 259–290 in D. F. Sax, J. J. Stachowicz, and S. D. Gaines, eds. *Species invasions: insights into ecology, evolution, and biogeography*. Sinauer, Sunderland, MA.
- Hovestadt, T., S. Messner, and H. J. Poethke. 2001. Evolution of reduced dispersal mortality and “fat-tailed” dispersal kernels in autocorrelated landscapes. *Proceedings of the Royal Society B: Biological Sciences* 268:385–391.
- Johnson, D. M., A. M. Liebhold, P. C. Tobin, and O. N. Bjornstad. 2006. Allee effects and pulsed invasion by the gypsy moth. *Nature* 444:361–363.
- Kearney, M., and W. P. Porter. 2004. Mapping the fundamental niche: physiology, climate, and the distribution of a nocturnal lizard. *Ecology* 85:3119–3131.
- Kokko, H., and A. Lopez-Sepulcre. 2006. From individual dispersal to species ranges: perspectives for a changing world. *Science* 313:789–791.
- Kot, M., M. A. Lewis, and P. van den Driessche. 1996. Dispersal data and the spread of invading organisms. *Ecology* 77:2027–2042.
- Kun, A., and I. Scheuring. 2006. The evolution of density-dependent dispersal in a noisy spatial population model. *Oikos* 115:308–320.
- Lampo, M., and G. A. De Leo. 1998. The invasion ecology of the

- toad *Bufo marinus*: from South America to Australia. *Ecological Applications* 8:388–396.
- Lewontin, R. C. 1965. Selection for colonizing ability. Pages 79–94 in H. Baker and G. Stebbins, eds. *The genetics of colonizing species*. Academic Press, New York.
- Mack, R. N., D. Simberloff, W. M. Lonsdale, H. Evans, M. Clout, and F. Bazzaz. 2000. Biotic invasions: causes, epidemiology, global consequences and control. *Ecological Applications* 10:689–710.
- Neubert, M. G., and H. Caswell. 2000. Demography and dispersal: calculation and sensitivity analysis of invasion speed for structured populations. *Ecology* 81:1613–1628.
- Phillips, B. L., G. P. Brown, J. K. Webb, and R. Shine. 2006. Invasion and the evolution of speed in toads. *Nature* 439:803.
- Phillips, B. L., G. P. Brown, M. Greenlees, J. K. Webb, and R. Shine. 2007. Rapid expansion of the cane toad (*Bufo marinus*) invasion front in tropical Australia. *Austral Ecology* 32:169–176.
- Sabath, M. D., W. C. Boughton, and S. Easteal. 1981. Expansion of the range of the introduced toad *Bufo marinus* in Australia 1935–1974. *Copeia* 1981:676–680.
- Shigesada, N., and K. Kawasaki. 1997. *Biological invasions: theory and practice*. Oxford Series in Ecology and Evolution. Oxford, Oxford University Press.
- Skellam, J. G. 1951. Random dispersal in theoretical populations. *Biometrika* 38:196–218.
- Taylor, C. M., and A. Hastings. 2005. Allee effects in biological invasions. *Ecology Letters* 8:895–908.
- Thomas, C. D., A. Cameron, R. E. Green, M. Bakkenes, L. J. Beaumont, Y. C. Collingham, B. F. N. Erasmus, et al. 2004. Extinction risk from climate change. *Nature* 427:145–148.
- Tobin, P. C., S. L. Whitmire, D. M. Johnson, O. N. Bjornstad, and A. M. Liebhold. 2007. Invasion speed is affected by geographical variation in the strength of Allee effects. *Ecology Letters* 10:36–43.
- Travis, J. M. J. 2003. Neighbourhood size, dispersal distance and the complex dynamics of the spatial Ricker model. *Population Ecology* 45:227–237.
- Travis, J. M. J., and C. Dytham. 2002. Dispersal evolution during invasions. *Evolutionary Ecology Research* 4:1119–1129.
- Urban, M. C., B. L. Phillips, D. K. Skelly, and R. Shine. 2007. The cane toad's (*Chaunus [Bufo] marinus*) increasing ability to invade Australia is revealed by a dynamically updated range model. *Proceedings of the Royal Society B: Biological Sciences* 274:1413–1419.
- . 2008. A toad more traveled: the heterogeneous invasion dynamics of cane toads in Australia. *American Naturalist* 171: E134–E148.

Symposium Editor: Trevor D. Price



Cane toads have evolved increased dispersal ability as a consequence of their invasion of northern Australia.